Published on 15 September 2020. Downloaded by Universidade Federal do Rio Grande do Sul on 2/10/2021 7:31:45 PM.

PCCP

ROYAL SOCIETY OF CHEMISTRY

PAPER

View Article Online
View Journal | View Issue

Check for updates

Cite this: *Phys. Chem. Chem. Phys.*, 2020, **22**, 24712

Charge regulation of colloidal particles in aqueous solutions

Amin Bakhshandeh, [a] Derek Frydel[b] and Yan Levin *[a]

Received 7th July 2020,
Accepted 10th September 2020

DOI: 10.1039/d0cp03633a

rsc.li/pccp

We study the charge regulation of colloidal particles inside aqueous electrolyte solutions. To stabilize a colloidal suspension against precipitation, colloidal particles are synthesized with either acidic or basic groups on their surface. On contact with water, these surface groups undergo proton transfer reactions, resulting in colloidal surface charge. The charge is determined by the condition of local chemical equilibrium between hydronium ions inside the solution and at the colloidal surface. We use a model of Baxter sticky spheres to explicitly calculate the equilibrium dissociation constants and to construct a theory which is able to quantitatively predict the effective charge of colloidal particles with either acidic or basic surface groups. The predictions of the theory for the model are found to be in excellent agreement with the results of Monte Carlo simulations. This theory is further extended to treat colloidal particles with a mixture of both acidic and basic surface groups.

I. Introduction

Aqueous solutions are of great importance in biology and chemistry.[1–4] In many cases such solutions are ionic. The long-range Coulomb interaction between charged particles is the main source of difficulty for exploring the thermodynamics of such systems.[5–11] Because of organic functional groups, many surfaces and membranes acquire surface charge when placed in water. From their interaction with water and an acid or a base these functional groups can either lose or gain a proton, thereby becoming charged.[12,13] The amount of charge gained in this process depends on the pH of the solution[14,15] and the process is known as charge regulation (CR).[16–32] CR is of great importance in colloidal science, biology, and chemistry[33–61] and is responsible for the stability of many different systems.[62–71]

The concept of charge regulation was first described by Linderstrøm-Lang and later developed by many other researchers.[20,72–77] The first quantitative implementation of charge regulation was performed by Ninham and Parsegian (NP)[78] who combined the idea of local chemical equilibrium with the Poisson–Boltzmann theory introduced by Gouy and Chapman sixty years earlier.[79,80] The fundamental assumption of the NP theory is that the bulk association constants can be used to study proton transfer reactions with the surface adsorption sites. Within the NP approach the bulk concentration of hydronium ions is replaced by the local density determined self consistently by the Boltzmann distribution,

$$c_{H^+}^{surf} = c_{H_3O^+}^{bulk} \exp(-\beta\phi_0), \tag{1}$$

where $\beta = 1/k_BT$ and ϕ_0 is the electrostatic surface potential.

The NP theory relies on the Poisson–Boltzmann equation with the CR implemented as a new boundary condition. The two parameters that determine the boundary conditions are the equilibrium constant of the chemical reaction taking place at the surface, and the surface density of the chemical groups. Within the NP model, the surface is homogeneous, therefore, the model ignores the discrete structure of surface chemical groups. Another assumption is that the equilibrium constant is defined in terms of the concentrations of the reacting species rather than their activities. The validity of this assumption needs to be tested, since the concentration of hydronium ions can be quite large near a charged surface. Finally, the value of the equilibrium constant at the surface is assumed to be the same as for the reaction in the bulk. This is clearly far from obvious.

In this paper we will focus on spherical colloidal particles with acidic and basic surface groups. If a colloidal particle has N_{site} basic functional groups on its surface then the effective surface charge within the NP theory is found to be

$$\sigma = \frac{K_{Bulk} N_{site} q c_a e^{-\beta\phi_0}}{4\pi(a + r_{ion})^2 (1 + K_{Bulk} c_a e^{-\beta\phi_0})}, \tag{2}$$

where a is the colloidal radius and c_a is the bulk concentration of the strong acid. On the other hand if the surface has N_{site}

[a] *Instituto de Física, Universidade Federal do Rio Grande do Sul, Caixa Postal 15051, CEP 91501-970, Porto Alegre, RS, Brazil. E-mail: amin.bakhshandeh@ufrgs.br, levin@if.ufrgs.br*
[b] *Department of Chemistry, Federico Santa Maria Technical University, Campus San Joaquin, 7820275, Santiago, Chile. E-mail: derek.frydel@usm.cl*

This journal is © the Owner Societies 2020

Published on 15 September 2020. Downloaded by Universidade Federal do Rio Grande do Sul on 2/10/2021 7:31:45 PM.

acidic groups, the effective surface charge is

$$\sigma = -\frac{N_{\text{site}} q}{4\pi(a + r_{\text{ion}})^2} + \frac{K_{\text{Bulk}} N_{\text{site}} q c_{\text{a}} \mathrm{e}^{-\beta\phi_0}}{4\pi(a + r_{\text{ion}})^2 (1 + K_{\text{Bulk}} c_{\text{a}} \mathrm{e}^{-\beta\phi_0})}, \quad (3)$$

where K_{Bulk} is the bulk equilibrium association constant, which is the inverse of the acid dissociation constant K_{a}, and q is the elementary proton charge. The electrostatic surface potential ϕ_0 must be calculated self-consistently by combining these expressions with the mean-field Poisson–Boltzmann equation.

The fundamental ingredient of the NP theory is the equilibrium constant. In the original approach the equilibrium constant for the active sites on the colloidal surface was assumed to be the same as that of the bulk solution, however, in the latter studies the equilibrium constant was treated as a fitting parameter. Clearly this is not very satisfactory, since it does not allow us to explicitly probe the validity of the theory. Although, the NP theory was a pioneering first step in understanding charge regulation in colloidal systems, in the absence of an explicit model on which the theory could be tested, the validity of the underlying approximations of the theory remains unclear. A different approach was recently advocated by Bakhshandeh *et al.* in which a specific model of association was used to calculate exactly the bulk equilibrium constant for acids.[16] The same acidic groups were then placed on top of a spherical colloidal particle and the density profiles for hydronium cations and the corresponding anions were calculated exactly – within this model – using Monte Carlo simulations. Knowledge of the exact equilibrium constant allowed us to explicitly compare the results of simulations with the NP theory. It was found that the NP approach deviated significantly from the predictions of simulations. For the specific case of acidic surface groups, the study in ref. 16 then introduced an alternative approach which was found to be in excellent agreement with the Monte Carlo simulations. The objective of this paper is to extend the results of ref. 16 to colloidal particles with basic surface groups, as well to the particles containing a mixture of basic and acidic surface groups.

We should note that the present theory applies directly only to the specific model of chemical association described below. There are two levels of approximation that we use: 1 – the microscopic model of acid–base association in terms of Baxter sticky spheres, and 2 – the approximations used to theoretically solve the model. The advantage of this two-step approach is that the theory can be tested against an ''exact'' solution of the microscopic model obtained using computer simulations. This allows us to separate the possible shortfalls of the theory from those of the microscopic model. If the theory agrees with the ''exact'' solution of the model, any shortfalls can then be attributed to the microscopic model of association and not to the approximations which had to be made to solve the model. The disadvantage of such an approach is that the theory that we develop applies only to the specific microscopic model of acid/base equilibrium and is not generally universal. This, however, is the problem with any microscopic theory which does not explicitly take into account all the quantum effects associated with the charge transfer at the interface. In the absence of such ''complete'' theory, we expect that the approach advocated in the present paper will help to shed interesting new light on the mechanisms of charge regulation of nanoparticles and colloidal suspensions, and in particular on the applicability of mean-field theories to study this intrinsically strong-coupling problem.

There are several possibilities for a colloidal surface to acquire charge. The acidic functional groups, such as carboxyl COOH, can become dissociated due to the following reaction

$$\mathrm{HA} + \mathrm{H_2O} \rightleftarrows \mathrm{H_3O^+} + \mathrm{A^-}, \quad (4)$$

resulting in a negatively charged surface. Alternatively, basic functional groups, which originally are not charged, can gain protons from hydronium ions and acquire a positive charge,

$$\mathrm{B} + \mathrm{H_3O^+} \rightleftarrows \mathrm{H_2O} + \mathrm{HB^+}. \quad (5)$$

One example of such a functional group is amine NH_2.

This paper is organized as follows. In Section II, we introduce a model of colloidal particles with sticky sites and present the details of Monte Carlo simulations. In Section III, we show how the equilibrium association constant can be calculated for sticky ions. In Section IV, we present a model for a uniformly sticky colloidal particle. In Section V, this model is extended to account for discrete basic surface groups, and in Sections VI and VII to discrete acidic groups. In Section VIII, we consider particles with a mixture of both basic and acidic surface groups and in Section IX, we present our conclusions.

II. Theoretical background and Monte Carlo simulation details

A. Theoretical background

To study the charge regulation of a colloidal surface we use a model of Baxter sticky spheres.[18,81,82] The sticky potential was previously used to study gelation in globular proteins,[83,84] chemical association in weak acid–base reactions,[85] and sticky-charged wall models.[86–89] In our model, sticky interactions take on a physical interpretation of a chemical bond between protons and acid/base groups. This is not the first time that a sticky interaction is used to model a chemical bond to capture some aspects of quantum mechanics in an otherwise classical description. This idea has been around for some time and reaches back to 1980 in particular, the work of Blum and Herrera,[85,86] and Werthaim[90] for directional chemical bonding. Sticky interactions continue to this day being an important part of soft-matter modeling.[91] In the present work, sticky interactions, and their quantum-chemical interpretation, will be used to study the charge regulation of nanoparticles with surface acid and base groups. The results obtained, therefore, are only valid within the specific microscopic model. The model, of course, can be extended and modified to represent a different charge regulated system. For example, directional chemical bonding could be introduced by making a sphere sticky in specific regions only. The size and shape of an absorbing molecule could be changed. These alternatives are not explored in the present work.

The hydronium ion can become adsorbed on an acidic or a basic functional group to form a molecule H^+A^- or H^+B,

Published on 15 September 2020. Downloaded by Universidade Federal do Rio Grande do Sul on 2/10/2021 7:31:45 PM.

respectively. To model the binding between H^+ and A^- or B we use an attractive square well potential with a repulsive hard core.[16,18] The first component of the interaction potential is the hard-core repulsion,

$$u_{\rm hs}(r) = \begin{cases} \infty, & r < d, \\ 0, & r > d, \end{cases} \tag{6}$$

where d is the diameter of particles. The second component is a narrow attractive well,

$$u_{\rm well}(r) = \begin{cases} 0, & r < d, \\ -\varepsilon, & d < r < d + \Delta, \\ 0, & r > d + \Delta. \end{cases} \tag{7}$$

To generalize the model, we also include a soft potential $u_{\rm sf}(r > d)$, so that the total pair potential becomes $u_{\rm tot} = u_{\rm hs} + u_{\rm well} + u_{\rm sf}$,

$$u_{\rm tot}(r) = \begin{cases} \infty, & r < d, \\ -\varepsilon + u_{\rm sf}(r), & d < r < d + \Delta, \\ u_{\rm sf}(r), & r > d + \Delta. \end{cases} \tag{8}$$

We note that the soft potential $u_{\rm sf}(r)$ is effective from $r = d$, as illustrated in Fig. 1.

For illustration, we consider a very simple scenario comprised of two particles interacting *via* a pair potential in eqn (8) and confined to a spherical region of radius R. To make the demonstration even simpler, one particle is fixed at the origin and only the second particle is free. The resulting partition function has two parts,

$$\begin{aligned} \mathcal{Z} &= 4\pi \int_d^R r^2 e^{-\beta[u_{\rm well}(r)+u_{\rm sf}(r)]} dr \\ &= 4\pi e^{\beta\varepsilon} \int_d^{d+\Delta} r^2 e^{-\beta u_{\rm sf}(r)} dr + 4\pi \int_{d+\Delta}^R r^2 e^{-\beta u_{\rm sf}(r)} dr. \end{aligned} \tag{9}$$

Assuming a small Δ, we can expand Z in Δ, yielding

$$\begin{aligned} \mathcal{Z} &= 4\pi d^2 e^{\beta\varepsilon} e^{-\beta u_{\rm sf}(d)} \left[\Delta\left(1 - e^{-\beta\varepsilon}\right) \right. \\ &\quad \left. + \left(\frac{1}{d} - \frac{1}{2}\frac{d\beta u_{\rm sf}(r)}{dr}\Big|_{r=d}\right)\Delta^2 + \cdots\right] \\ &\quad + 4\pi \int_d^R r^2 e^{-\beta u_{\rm sf}(r)} dr. \end{aligned} \tag{10}$$

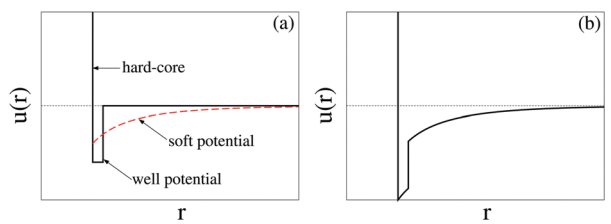

Fig. 1 Schematic representation of the sticky-hard-sphere potential plus soft interaction. The sticky part is represented as a narrow well potential; (a) depicts hard-core plus attractive well and soft potential separately, and (b) as a combination. An important observation is that the soft interaction is active within the attractive well.

In the limit $\Delta \to 0$ only the last term does not vanish. However, if, at the same time as $\Delta \to 0$, $\varepsilon \to \infty$, then some of the expansion terms must also be retained. The correct way to carry out the limit is to have $\Delta e^{\beta\varepsilon}$ = constant, which is referred to as the Baxter limit,[81] and yields

$$\lim_{\substack{\Delta\to 0 \\ \varepsilon\to\infty}} \mathcal{Z} = 4\pi d^2 l_{\rm g} e^{-\beta u_{\rm sf}(d)} + 4\pi \int_d^R r^2 e^{-\beta u_{\rm sf}(r)} dr, \tag{11}$$

where we introduced the "sticky length" defined as

$$l_{\rm g} = \lim_{\substack{\varepsilon\to\infty \\ \Delta\to 0}} \Delta e^{\beta\varepsilon}. \tag{12}$$

Of great concern for simulations is the width Δ of the well potential, since in practice the exact Baxter limit cannot be attained and Δ must remain finite. To estimate what is a sufficiently small value of Δ, we consider the previous simple system with $u_{\rm sf} = 0$, for which the exact partition function is

$$\mathcal{Z} = 4\pi d^2 l_{\rm g}\left[1 + \frac{\Delta}{d} + \frac{1}{3}\left(\frac{\Delta}{d}\right)^2\right] + \frac{4\pi R^3}{3}\left[1 - \left(\frac{d+\Delta}{R}\right)^3\right]. \tag{13}$$

If we ignore the second term in square brackets, assuming $R \gg d$, we conclude that the well potential becomes sticky if $\Delta/d \ll 1$. In practice, we find that $\Delta/d \approx 0.01$ is sufficiently small to suppress most contributions of finite Δ.

The Baxter sticky potential may appear analogous to a delta function potential often used in quantum mechanics. This, however, is misleading. The well potential in eqn (7) transforms into the delta function in the limits $\Delta \to 0$ and $\varepsilon \to \infty$, while the product $\Delta\varepsilon$ is held fixed. On the other hand, the Baxter limit requires that $\Delta e^{\beta\varepsilon}$ remains constant. To see this more clearly[18] we define

$$f(r) = \begin{cases} \dfrac{1}{\Delta}, & d \le r \le d + \Delta, \\ 0, & r < d \text{ or } r > d + \Delta. \end{cases} \tag{14}$$

The Boltzmann factor then can be written as

$$e^{-\beta u_{\rm well}(r)} = 1 + \Delta(e^{\beta\varepsilon} - 1) f(r), \tag{15}$$

in which the Baxter limit reduces to

$$\lim_{\substack{\varepsilon\to\infty \\ \Delta\to 0}} e^{-\beta u_{\rm well}(r)} = 1 + l_{\rm g}\delta(r - d), \tag{16}$$

with the sticky length given by $l_{\rm g} \equiv \Delta(e^{\beta\varepsilon} - 1)$. In the Baxter limit the -1 in the definition of $l_{\rm g}$ can be neglected, however, in the simulations with finite Δ we will use the exact expression for $l_{\rm g}$. The sticky potential itself is then

$$\beta u_{\rm well}(r) = -\ln[1 + l_{\rm g}\delta(r - d)], \tag{17}$$

which shows that it is weaker than the delta function potential. Indeed, a delta function potential would result in an irreversible association between the sticky spheres. Finally, we note that if the expression (16) is used in the partition function eqn (9), we will arrive directly at eqn (11).

 This journal is © the Owner Societies 2020

Published on 15 September 2020. Downloaded by Universidade Federal do Rio Grande do Sul on 2/10/2021 7:31:45 PM.

B. Monte Carlo simulations details

We are now in a position to implement numerical simulations. The simulations are performed inside a spherical Wigner–Seitz (WS) cell of radius R. A spherical colloidal particle of radius a is placed in the center of the WS cell. The radius of the cell is determined by the colloidal volume fraction of the suspension, $\varphi_c = a^3/R^3$. The motivation for using WS is that for a low salt concentration, the colloidal system may crystallize, in which case the thermodynamics will be very well described by the WS cell model, with a Donnan potential used to control the charge neutrality. In fact, even for the disordered state the WS approach to thermodynamics is found to lead to osmotic pressures in excellent agreement with experiments.[92] In a sense, the many body colloid–colloid interactions in the grand-canonical ensemble are all included through the boundary conditions of vanishing electric field at the WS cell boundary.

The colloidal particle has N_{site} adsorption sites randomly distributed over its surface. Each adsorption site is a sphere of diameter d, see Fig. 2. If an active site is basic – has zero charge – it interacts with the hydronium ions through the hard core and the Baxter sticky potential, eqn (8). On the other had if the site is acidic – has charge $-q$, where q is the proton charge – in addition to the Baxter and hard core interactions, there is also a long range Coulomb potential between the adsorption site and all the ions inside the simulation cell. In this work all the ions and the adsorption sites have a diameter of 4 Å and the colloidal particle has a radius of a = 100 Å.

The system is connected to a reservoir of strong acid at concentration 10^{-pH}, and a reservoir of 1 : 1 strong electrolyte at concentration c_s.

The solvent is considered to be of uniform dielectric permittivity $\varepsilon_w = 80\varepsilon_0$ and the Bjerrum length is $\lambda_B = q^2/\varepsilon_w k_B T$ = 7.2 Å. The total interaction potential is

$$U = \sum_{i>j} \frac{q_i q_j}{\varepsilon_w |\mathbf{r}_i - \mathbf{r}_j|} + {\sum}' u_{well}(\mathbf{r}_i), \qquad (18)$$

where the first sum is over all the charged particles, including the adsorption sites, and the second sum is for the sticky interaction between the hydronium ions and the adsorption sites. The hard-core interaction between ions, sites, and colloidal surface is implicit. The restriction on the second sum indicated by the prime is due to the fact that each functional site can adsorb at most one hydronium ion. This is the case for carboxyl or amine groups. Therefore, once there is a hydronium ion within the distance Δ of the adsorption site, the short range sticky potential of this site with other hydronium ions is switched off. In this paper we will not consider more complicated metal oxide ions which can adsorb more than one proton. To perform simulations we used the Metropolis algorithm.[93] For large WS cells, when a system establishes a well-defined bulk concentration far from the colloidal surface, we can use canonical Monte Carlo simulations.[94] For large colloidal volume fractions, when WS is small and bulk concentration is not reached inside the cell, we use the grand canonical Monte Carlo simulations.[94] This is done in order to have well defined reservoir concentrations of acid c_a and salt c_s, which are necessary to compare the theory with the simulations. In both types of simulations we have used 5×10^6 MC steps for equilibration and 10^4 steps for production.

We first check the convergence of MC results to the Baxter sticky limit by studying systems with different values of Δ and ε, while keeping fixed the sticky length l_g. Fig. 3 shows the rapid convergence to the Baxter limit, with a decreasing value of Δ.

III. Equilibrium constant for particles interacting *via* a pair potential

To connect the simulations presented in the previous section with the NP theory we must relate the sticky length to the bulk association constant.

A. Neutral pairs

We first consider a general two-component system of sticky spheres. To avoid confusion with previous labels, we designate

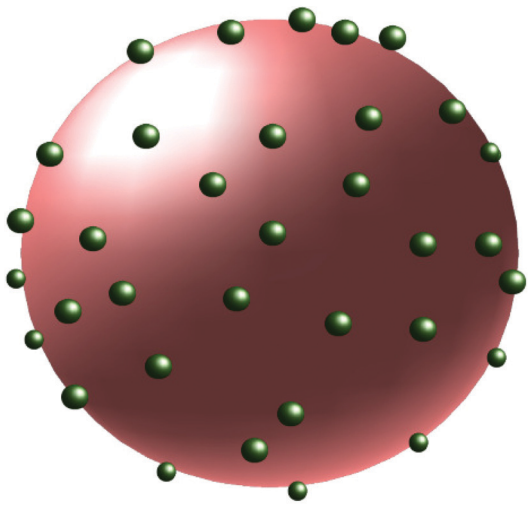

Fig. 2 The Baxter's sticky spherical sites on the colloidal surface.

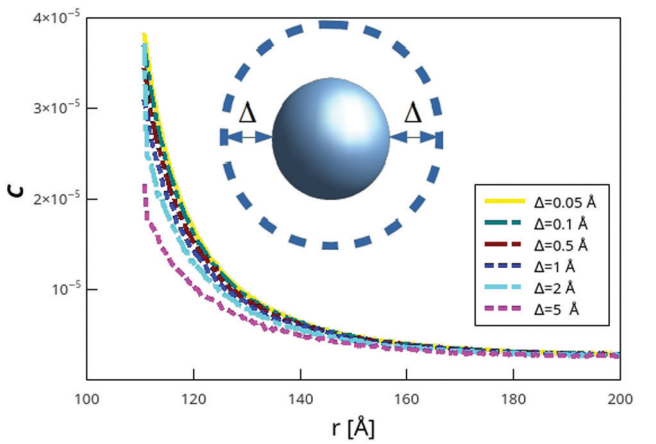

Fig. 3 The density profiles of ions for different size Δ and fixed l_g = 109.9 Å. The density is plotted in terms of the number of particles per Å^3.

Published on 15 September 2020. Downloaded by Universidade Federal do Rio Grande do Sul on 2/10/2021 7:31:45 PM.

the ''atoms'' of each species as X and Y. The interaction between atoms of the same species is

$$u_{xx}(r) = u_{yy}(r) = u_{\mathrm{hs}}(r) + u_{\mathrm{sf1}}(r), \tag{19}$$

and between the atoms of different species is

$$u_{xy}(r) = u_{\mathrm{hs}}(r) + u_{\mathrm{sf2}}(r) + u_{\mathrm{well}}(r), \tag{20}$$

This is the, so called, ''physical picture'', in which only atoms exist. Alternatively, we can regard two atoms X and Y in contact to form a molecule XY. This corresponds to the ''chemical picture'', see Fig. 4 for illustration. In the chemical picture, we have free atoms X and Y, and molecules XY which are in ''chemical'' equilibrium,[95]

$$X + Y \rightleftharpoons XY. \tag{21}$$

At most two atoms X and Y are permitted to interact *via* a sticky potential. Without this restriction, one has to account for the presence of triplets XYX, quartets $XYXY$, and other higher order formations, together with their corresponding chemical reactions.

To obtain the equilibrium constant for the chemical reaction in eqn (21) we compare the equations of state calculated using the physical and the chemical pictures. Clearly the osmotic pressure calculated using the two interpretations of the same physical reality has to be same.

Within the physical interpretation, the system is comprised of two types of atoms, X and Y, and the formation of pairs XY is devoid of any special meaning. The virial expansion of the osmotic pressure up to second order in bulk concentration c_i is[96]

$$\beta P_{\mathrm{phys}} = c_x + c_y + B_{xx}{c_x}^2 + B_{yy}{c_y}^2 + 2B_{xy}c_xc_y + \ldots, \tag{22}$$

where B_{ij} are the second virial coefficients defined as

$$B_{ij} = 2\pi\int_0^\infty (1 - \mathrm{e}^{-\beta u_{ij}(r)})r^2\mathrm{d}r, \tag{23}$$

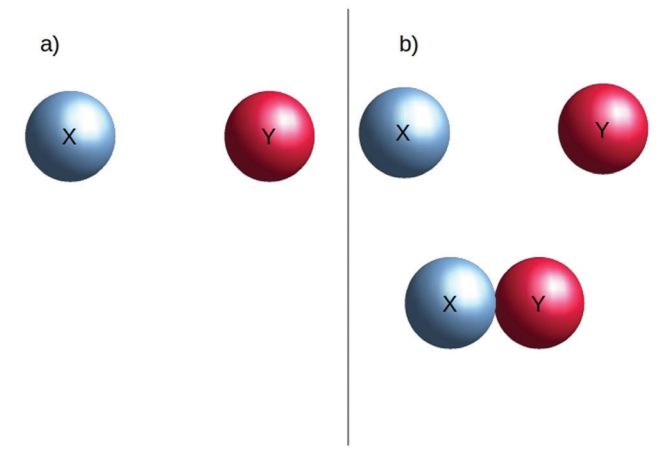

Fig. 4 The two representations correspond to (a) a physical and (b) a chemical interpretation.

and whose various contributions are

$$\begin{aligned} B_{xx} &= B_{yy} = B_{\mathrm{hs}} + B_{\mathrm{sf1}}, \\ B_{xy} &= B_{\mathrm{hs}} + B_{\mathrm{st}} + B_{\mathrm{sf2}}, \end{aligned} \tag{24}$$

which, after evaluation, become

$$\begin{aligned} B_{\mathrm{hs}} &= \frac{2\pi d^3}{3}, \\ B_{\mathrm{st}} &= -2\pi l_{\mathrm{g}} d^2 \mathrm{e}^{-\beta u_{\mathrm{sf2}}(d)}, \\ B_{\mathrm{sf1}} &= 2\pi\int_d^\infty (1 - \mathrm{e}^{-\beta u_{\mathrm{sf1}}(r)})r^2\mathrm{d}r, \\ B_{\mathrm{sf2}} &= 2\pi\int_d^\infty (1 - \mathrm{e}^{-\beta u_{\mathrm{sf2}}(r)})r^2\mathrm{d}r, \end{aligned} \tag{25}$$

where B_{st} was evaluated using the Boltzmann factor in eqn (16). Inserting these contributions into the expansion in eqn (22) yields

$$\beta P_{\mathrm{phys}} = c_x + c_y + B_{\mathrm{hs}}(c_x + c_y)^2 + B_{\mathrm{sf1}}({c_x}^2 + {c_y}^2) + 2B_{\mathrm{sf2}}c_xc_y + 2B_{\mathrm{st}}c_xc_y + \ldots, \tag{26}$$

where the first line is the ideal-gas contribution, the second line is the second order correction due to hard-core and soft interactions, and the third line is the second order correction due to the sticky potential.

To formulate the equation of state within the chemical picture, we need to define the concentrations of free atoms X, Y, and of molecules XY, designated by the superscript *:

$$\begin{aligned} c_x^* &= c_x - c_{xy}^*, \\ c_y^* &= c_y - c_{xy}^*, \\ c_{xy}^* &= K_{\mathrm{Bulk}}c_x^*c_y^*, \end{aligned} \tag{27}$$

where the last equation was obtained using the definition of the equilibrium constant of the reaction in eqn (21),

$$K_{\mathrm{Bulk}} = \frac{c_{xy}^*}{c_x^*c_y^*}, \tag{28}$$

valid in the dilute limit where activities are approximated by concentrations. To second order in concentrations c_i, eqn (27) can be written as

$$\begin{aligned} c_x^* &= c_x - K_{\mathrm{Bulk}}c_xc_y + \ldots, \\ c_y^* &= c_y - K_{\mathrm{Bulk}}c_xc_y + \ldots, \\ c_{xy}^* &= K_{\mathrm{Bulk}}c_xc_y + \ldots \end{aligned} \tag{29}$$

In the chemical picture, the interactions between free atoms X and Y do not include sticky interaction,

$$u'_{xy}(r) = u_{\mathrm{hs}}(r) + u_{\mathrm{sf2}}(r).$$

which acts only within a molecule XY. Without the sticky interaction, the modified second virial coefficient in the chemical interpretation is

$$B'_{xy} = B_{\mathrm{hs}} + B_{\mathrm{sf2}}. \tag{30}$$

This journal is © the Owner Societies 2020

Published on 15 September 2020. Downloaded by Universidade Federal do Rio Grande do Sul on 2/10/2021 7:31:45 PM.

The osmotic pressure up to second order in concentrations c_i is then

$$\beta P_{\text{chem}} = c_x^* + c_y^* + c_{xy}^* + B_{xx}c_x^{*2} + B_{yy}c_y^{*2} + 2B'_{xy}c_x^*c_y^* + \dots. \tag{31}$$

The terms

$$2B_{x,xy}c_x^*c_{xy}^* + 2B_{y,xy}c_y^*c_{xy}^* + B_{xy,xy}{c_{xy}^*}^2, \tag{32}$$

that are second order in c_i^* are omitted since, due to $c_{xy}^* \approx K_{\text{Bulk}}c_xc_y$ in eqn (29), they are of higher order in c_i. Using formulae in eqn (29), and substituting for the coefficients B_{ij}, eqn (31) becomes

$$\beta P_{\text{chem}} = c_x + c_y + B_{\text{hs}}(c_x + c_y)^2 + B_{\text{sf1}}({c_x}^2 + {c_y}^2) + 2B_{\text{sf2}}c_xc_y - K_{\text{Bulk}}c_xc_y + \dots, \tag{33}$$

Setting $P_{\text{phys}} = P_{\text{chem}}$, and matching the terms of the same order yields

$$K_{\text{Bulk}} = -2B_{\text{st}} = 4\pi l_g d^2 \mathrm{e}^{-\beta u_{\text{sf2}}(d)}, \tag{34}$$

We note that the above derivation assumes a dilute limit, where the definition of K_{Bulk} in eqn (28) and the second order expansion of βP are valid. The result in eqn (34), however, is exact for any concentration. This is because the quantity K_{Bulk} itself is independent of concentrations. We simply took advantage of this fact and chose the limit where all the expressions are the simplest.

If we set $u_{\text{fs2}} = 0$, the equilibrium constant becomes

$$K_{\text{Bulk}} = 4\pi l_g d^2, \tag{35}$$

which is appropriate for the pair formation between bases and hydronium ions. On the other hand, as we will see in the following section, eqn (34) with u_{sf2} corresponding to the Coulomb potential will be appropriate for the weak acid-hydronium equilibrium constant.

B. Charged pairs

In bulk, the acid "molecule" dissociates resulting in a hydronium ion and a corresponding anion:

$$\text{HA} \rightleftarrows \text{H}^+ + \text{A}^-, \tag{36}$$

The thermodynamics of bulk electrolytes, even without covalent bonding between the ions, is complicated by the divergence of the virial expansion due to the long range nature of the Coulomb interaction. Instead a certain class of perturbative diagrams must be summed together to obtain a finite result.[96] This leads to a non-analytic term in the density expansion of the osmotic pressure which scales with the electrolyte concentration as $c^{3/2}$. The next order term which scales as c^2 can be interpreted as the result of Bjerrum anion–cation pair formation. In the case of purely electrostatic interactions, the equilibrium constant for such cluster formation was derived by Ebeling[97] considering the exact density expansion of the equation of state up to $\mathcal{O}(c^{5/2})$.[98] The Ebeling equilibrium constant is:

$$K_{\text{Eb}} = 8\pi d^3\left\{\frac{1}{12}b^3[\text{Ei}(b) - \text{Ei}(-b)] - \frac{1}{3}\cosh b - \frac{1}{6}b\sinh b - \frac{1}{6}b^2\cosh b + \frac{1}{3} + \frac{1}{2}b^2\right\}, \tag{37}$$

where $b = \dfrac{\lambda_B}{d}$. For large values of b (strong coupling limit), the equilibrium constant can be expanded asymptotically to give:

$$K_{\text{Eb}} = 4\pi a^3\frac{\mathrm{e}^b}{b}\left(1 + \frac{4}{b} + \frac{4\times 5}{b^2} + \frac{4\times 5\times 6}{b^3} + \dots\right). \tag{38}$$

This may be compared with the Bjerrum phenomenological association constant for the formation of anion–cation pairs

$$K_{\text{Bj}} = 4\pi\int_d^{R_{\text{Bj}}} \mathrm{e}^{\frac{\lambda_B}{r}} r^2\mathrm{d}r, \tag{39}$$

where $R_{\text{Bj}} = \lambda_B/2$ is the Bjerrum cutoff. In the strong coupling limit (low temperatures), K_{Bj} is completely insensitive to the precise value of cutoff R_{Bj}.[5] Furthermore, the low temperature expansions for K_{Eb} and K_{Bj} are found to be identical.[5] One can then interpret the Ebeling equilibrium constant as the analytic continuation of K_{Bj} over the full temperature range. With this observation it becomes easy to obtain the equilibrium constant for sticky electrolytes. In the spirit of Bjerrum, we then write

$$K_{\text{Bulk}} = 4\pi\int_d^{R_{\text{Bj}}} \mathrm{e}^{-\beta u_{\text{st}}(r) + \frac{\lambda_B}{r}} r^2\mathrm{d}r. \tag{40}$$

Using eqn (16) we obtain

$$K_{\text{Bulk}} = 4\pi\int_d^{R_{\text{Bj}}} \left[(1 + l_g\delta(r-d)\right]\mathrm{e}^{\frac{\lambda_B}{r}} r^2\mathrm{d}r, \tag{41}$$

which after integration yields,

$$K_{\text{Bulk}} = 4\pi d^2 l_g \mathrm{e}^b + \int_d^{R_{\text{Bj}}} \mathrm{e}^{\frac{\lambda_B}{r}} r^2\mathrm{d}r. \tag{42}$$

The validity of the above equation is extended beyond the strong coupling limit by replacing the integral with K_{Eb}. In the case of weak acids, large l_g, the first term will dominate eqn (42), so that the bulk equilibrium constant for a weak acid can be approximated by

$$K_{\text{Bulk}} = 4\pi d^2 l_g \mathrm{e}^b, \tag{43}$$

which is similar to eqn (34) of the previous section.

IV. Uniformly sticky colloid

To build a theory of charge regularization of colloidal particles we start with the simplest possible model in which the whole of the colloidal surface is sticky. A colloidal particle of radius a is placed at the center of a spherical WS cell of radius R. The density profiles of ions, then, satisfy the modified

Published on 15 September 2020. Downloaded by Universidade Federal do Rio Grande do Sul on 2/10/2021 7:31:45 PM.

Poisson–Boltzmann (mPB) equation:

$$\nabla^2\phi(r) = -\frac{4\pi}{\varepsilon_w}\sigma_0\delta(r-a-r_{ion}) - \frac{4\pi q}{\varepsilon_w}[c_{H^+}(r)+c_+(r)-c_-(r)], \quad (44)$$

where $\sigma_0 = 0$ if the surface groups are basic, and $\sigma_0 = -N_{sites}q/4\pi(a+r_{ion})^2$ if all the groups are acidic. The ionic concentrations are defined as:

$$c_{H^+}(r) = c_a e^{-\beta(u(r)+q\,\phi(r))} \quad (45)$$

$$c_+(r) = c_s e^{-\beta q\,\phi(r)} \quad (46)$$

$$c_-(r) = (c_a + c_s)e^{\beta q\,\phi(r)}, \quad (47)$$

where $u(r)$ is the sticky potential between the colloidal surface and a hydronium ion, $c_a = 10^{-pH}$ is the reservoir concentration of the acid, and c_s is the reservoir concentration of the 1 : 1 salt. We assume that both the acid and salt in the reservoir are strong electrolytes and are fully dissociated. Using eqn (16) we obtain $e^{-\beta(u(r)+q\,\phi(r))} = (1 - l_g\delta(r-a-r_{ion}))e^{-\beta q\,\phi(r)}$, which means that the surface density of adsorbed hydronium ions is:[16]

$$\sigma_{su} = qc_a l_g e^{-\beta q\phi_0}, \quad (48)$$

where $\phi_0 = \phi(a + r_{ion})$. The net surface charge density is then

$$\sigma_{net} = \sigma_0 + \sigma_{su}. \quad (49)$$

To calculate the ionic density profiles and the number of condensed hydronium ions we must now solve the PB equation

$$\nabla^2\phi(r) = \frac{8\pi q}{\varepsilon_w}(c_a + c_s)\sinh[\beta\phi(r)], \quad (50)$$

with the boundary conditions $\phi'(R) = 0$ and $\phi'(a + r_{ion}) = -4\pi\sigma_{net}/\varepsilon_w$. The calculation can be performed numerically using the 4th order Runge–Kutta, in which the value of the surface potential $\phi(a + r_{ion}) = \phi_0$ is adjusted based on the Newton–Raphson algorithm to obtain zero electric field at the cell boundary.

In reality, however, the whole of the colloidal surface is not uniformly sticky and hydronium ions can only adsorb onto special sites.[99] We now explicitly consider the modifications that must be made to the above theory in order to account for the discrete nature of adsorption sites.

V. Neutral functional groups

We first consider a colloidal particle with N_{site} neutral basic groups (sticky spheres) uniformly distributed on its surface. To simplify the geometry we will map the spherical sticky sites onto circular sticky patches of the same effective contact area. Since both hydronium and the adsorption sites are modeled by spheres of the same diameter d, the hard core repulsion between the colloidal surface and the hydronium ion restricts the effective contact area to $2\pi d^2$. Therefore, the patch radius must be

$$r_{patch} = \sqrt{2}d, \quad (51)$$

Compared to the situation discussed in the previous section in which the whole of the colloidal surface was sticky, the effective area on which hydronium ions can become adsorbed is significantly reduced in the case of discrete adsorption sites.[16] Nevertheless, we can still use the same approach as in Section 4, if the sticky length is rescaled as $l_g^{eff} = l_g\alpha_{eff}$, to account for the reduced adsorption area, where

$$\alpha_{eff} = \frac{N_{site}^{act}\pi {r_{patch}}^2}{4\pi(a+r_{ion})^2}, \quad (52)$$

is the fraction of the surface area occupied by the active sticky patches. Note that if hydronium is adsorbed onto a patch, this patch becomes inactive, preventing more than one hydronium ion from being adsorbed. The number of adsorbed hydronium ions is given by eqn (48) with l_g replaced by l_g^{eff}. As the process of adsorption progresses, the number of active sites decreases in such a way as

$$N_{site}^{act} = N_{site} - 4\pi(a+r_{ion})^2 c_a l_g^{eff} e^{-\beta\phi_0}, \quad (53)$$

resulting in a self-consistent equation for l_g^{eff}. Solving eqn (52) and (53), the effective sticky length is found to be

$$l_g^{eff} = \frac{l_g N_{site} {r_{patch}}^2}{4(a+r_{ion})^2\left(1 + l_g c_a e^{-\beta\phi_0}\pi {r_{patch}}^2\right)}. \quad (54)$$

The effective surface charge density which must be used as the boundary condition for the PB equation is then

$$\sigma_{eff} = qc_a l_g^{eff} e^{-\beta\phi_0} = \frac{qK_{Surf}N_{site}c_a e^{-\beta\phi_0}}{4\pi(a+r_{ion})^2(1+K_{Surf}c_a e^{-\beta\phi_0})}, \quad (55)$$

where $K_{Surf} = 2\pi l_g d^2 = K_{Bulk}/2$, where the bulk association constant is the same as in eqn (35).

We stress again that the bulk equilibrium constant K_{Bulk} is exact for the model of sticky hard spheres and does not depend on the density of the reactants. The higher order terms of the virial expansion, however, will modify the activity coefficients, so that in the law of mass action the concentrations will have to be replaced by the activities. Nevertheless, since the PB equation does not take into account ionic correlations, to remain consistent, the activity coefficients must also be set to unity. Solving eqn (50), with the boundary conditions $\phi'(R) = 0$ and $\phi'(a + r_{ion}) = -4\pi\sigma_{net}/\varepsilon_w$ we are able to obtain the density profile of ions around the colloidal particle.

To explore the range of validity of the theory we will compare it with the results of Monte Carlo simulations. We first consider colloidal particles with 300 and 600 active neutral basic sites and concentration of HCl set to 50 mM. In Fig. 5 and 6 we show the comparison between the simulation data, NP theory, and the present work, For these parameters the difference between the new theory and the NP approach is not very large, nevertheless it is clear that the simulation results are in a much better agreement with the theory developed in the present paper. The figures show that the density of free hydronium ions decreases near the colloidal surface. This is not surprising, since once some of the hydroniums have been adsorbed onto the neutral basic groups, the colloidal surface becomes positively charged and repels other cations. A more curious

 This journal is © the Owner Societies 2020

Published on 15 September 2020. Downloaded by Universidade Federal do Rio Grande do Sul on 2/10/2021 7:31:45 PM.

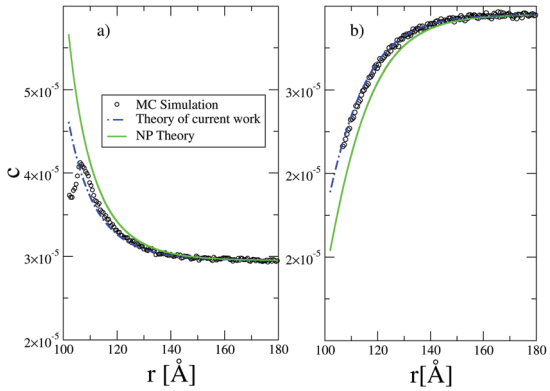

Fig. 5 Density profiles of hydronium and Cl^- measured in particles per Å^3. Symbols denote the simulation data and solid (green) and dashed (blue) lines are the predictions of the NP theory and of the theory developed in the present work, respectively. The parameters are a = 100 Å, R = 200 Å, and l_g = 109.97 Å. The colloidal particle has 300 neutral basic sites on its surface. The concentration of HCl is 50 mM. (a) Density profile of Cl^- and (b) density profile of hydronium.

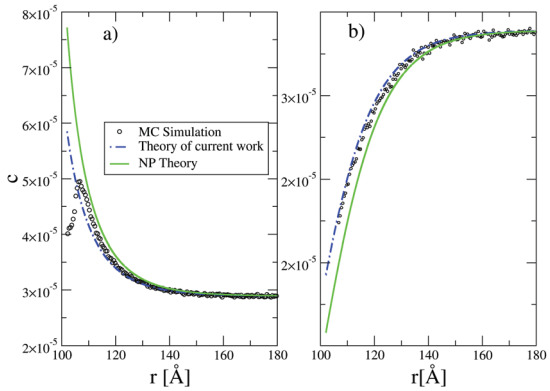

Fig. 6 Density profiles of hydronium and Cl^- measured in particles per Å^3. Symbols denote the simulation data and solid (green) and dashed (blue) lines are the predictions of the NP theory and of the theory developed in the present work, respectively. The parameters are a = 100 Å, R = 200 Å, and l_g = 109.97 Å. The colloidal particle has 600 basic sites on its surface. The concentration of HCl is 50 mM. (a) Density profile of Cl^- and (b) density profile of hydronium.

behavior is found for the anion Cl^-, the concentration of which shows a peak close to the surface, but then diminishes on further approach. The reason for this is that anions prefer to stay close to the adsorbed cations H^+, which in turn want to minimize the repulsive electrostatic energy between themselves as well as to maximize entropy. This favors the hydronium ions to be located at about 3 r_{ion} from the colloidal surface. This is precisely the position of the peak found in the density profile of anions. This fine detail, however, is beyond the scope of the present theory. Nevertheless the fact that the density profiles away from colloidal surface are perfectly described by the present theory implies that the prediction of the total number of adsorbed hydronium ions is correct, not withstanding the fine structure of ionic density profiles near the surface.

We next consider the effect of 1:1 salt on the charge regulation. We study a colloidal particle with 200 basic sites in the presence of HCl and NaCl, both at a concentration of 10 mM. We assume that both the acid and salt are completely ionized. The results of the theory and simulations are shown in Fig. 7.

Once again we see very good agreement between the present theory and the MC simulations.

In experiments, zeta potential is more easily determined than the effective charge. The definition of zeta potential, however, requires knowledge of the position of the slip plain. Nevertheless we expect that zeta potential will behave similarly to the electrostatic contact surface potential. In Fig. 8 and 9 we show the behavior of the surface potential and the effective charge Z_{eff} in units of charge q as a function of pH, for the present theory and NP theory, respectively and in Fig. 10, the behavior of the two as a function of salt concentration. We observe that the addition of 1:1 electrolyte diminishes the contact potential. This, in turn, lowers the electrostatic energy penalty for bringing hydronium ions to the colloidal surface, thus favoring their association with the active sites. Indeed, Fig. 10b shows that the effective charge of colloidal particles increases with the increasing salt concentration.

VI. Charged functional groups

We next consider a colloidal particle with N_{site} acidic surface groups each carrying a charge $-q$. If all the groups would be ionized, the particle would acquire a net charge $Q_0 = -N_{site}q$. The chemical equilibrium between hydronium and acid groups, however, reduces this value to $Q_{eff} = Q_0 + Q_{con}$, where

$$Q_{con} = 4\pi(a + r_{ion})^2 q c_a l_g^{eff} e^{-\beta q \varphi_0} \quad (56)$$

is the number of associated hydronium ions and φ_0 is the potential of mean force (PMF) – the work required to bring an

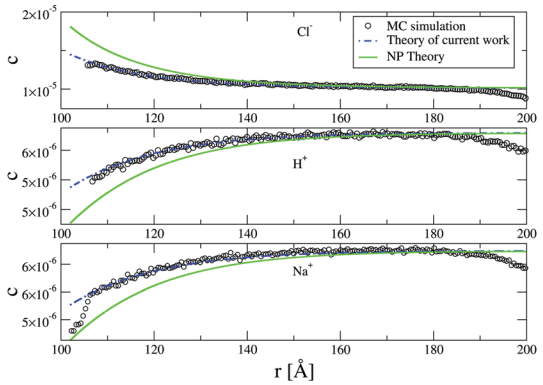

Fig. 7 Density profiles of hydronium, Cl^-, and Na^+ measured in particles per Å^3. Symbols denote the simulation data and solid (green) and dashed (blue) lines are the predictions of the NP theory and of the theory developed in the present work, respectively. The parameters are a = 100 Å, R = 200 Å, and l_g = 109.97 Å. The colloidal particle has 200 basic sites on its surface. The concentration of HCl and NaCl is 10 mM. The density C is in units of particles per Å^3.

Published on 15 September 2020. Downloaded by Universidade Federal do Rio Grande do Sul on 2/10/2021 7:31:45 PM.

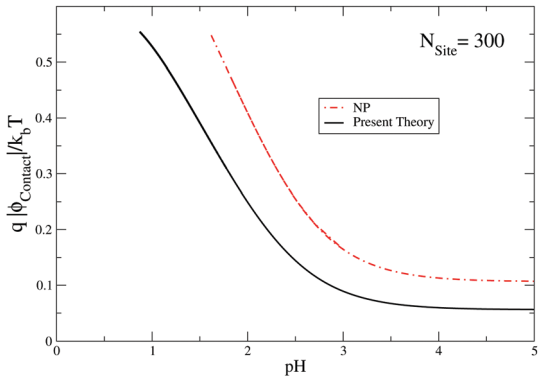

Fig. 8 Contact potential as a function of pH for the present theory and NP theory, respectively. The colloidal particle has 300 basic functional groups on its surface. The parameters are a = 100 Å, R = 200 Å, and l_g = 109.97 Å. There is no added salt.

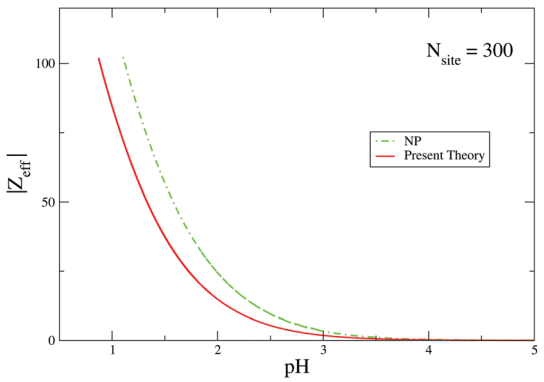

Fig. 9 Effective charge of colloidal particles in units of q as a function of pH for the present theory and NP theory, respectively. The colloidal particle has 300 basic active functional groups on its surface. The parameters are a = 100 Å, R = 200 Å, and l_g = 109.97 Å. There is no added salt.

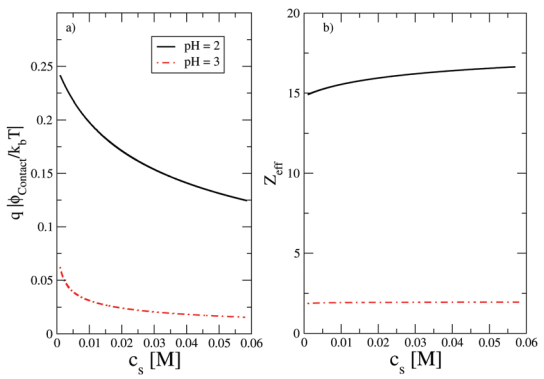

Fig. 10 (a) Contact potential and (b) the effective charge of colloidal particles in units of q as a function of salt concentration c_s (M) for different pH. The colloidal particle has 300 basic functional groups. The parameters are a = 100 Å, R = 200 Å, and l_g = 109.97 Å.

ion from the bulk to contact with one of the acidic groups. The PMF can be separated into a mean-field electrostatic potential ϕ_0 and a contribution from the discrete nature of surface charge groups μ_c^{qq},

$$\varphi_0 = \phi_0 + \mu_c^{qq}. \tag{57}$$

The value of l_g^{eff} is given by eqn (54) with the mean-field potential replaced by the PMF, $\phi_0 \to \varphi_0$. The effective surface charge density then reduces to

$$\sigma_{eff} = -\frac{N_{site} q}{4\pi(a + r_{ion})^2} + \frac{q K_{Surf}^a N_{site} c_a e^{-\beta\phi_0}}{4\pi(a + r_{ion})^2 \left(1 + K_{Surf}^a c_a e^{-\beta\phi_0}\right)} \tag{58}$$

where

$$K_{Surf}^a = \frac{K_{Bulk}^a}{2} e^{-b-\beta\mu_c^{qq}}, \tag{59}$$

and the bulk acid association constant K_{Bulk}^a is given by eqn (43). The term e^{-b} in eqn (59) discounts the direct Coulomb interaction between the hydronium ion and its adsorption site, which is already accounted for in the μ_c^{qq}.

VII. The effect of discrete charges

It is well known that the PB equation is very accurate for systems containing only 1 : 1 electrolyte. The mean-field nature of this equation is manifested by the complete neglect of ionic correlations, which are found to be small for aqueous solutions of monovalent ions.[5] However, in the case of acidic groups, hydronium ions will condense directly onto charged sites and the discrete nature of hydronium ions and the surface sites cannot be neglected for the associated ions. The free ions, however, can still be treated at the mean-field level.

To account for the discrete nature of surface groups, we add and subtract a uniform neutralizing background to the colloidal surface. The negative of the background can be combined with the mean-field electrostatic potential produced by the ions to yield the total mean-field electrostatic potential $\phi(r)$. The potential produced by the discrete surface charge and their neutralizing background, on the other hand, correspond to μ_c^{qq} defined in eqn (57). To calculate μ_c^{qq} we will ignore the curvature of the colloidal surface. Furthermore, we will suppose that the adsorption sites are uniformly distributed, forming a triangular lattice of spacing L.

We start by calculating the electrostatic potential produced by an infinite planar triangular array of charges, see Fig. 11. This potential must satisfy the Poisson equation

$$\nabla^2 G(\boldsymbol{r}) = -\frac{4\pi q}{\varepsilon_w} \sum_{n,m} \delta(z)\delta(\boldsymbol{\rho} - n\boldsymbol{a}_1 - m\boldsymbol{a}_2), \tag{60}$$

where z and $\boldsymbol{\rho} = x\hat{\boldsymbol{x}} + y\hat{\boldsymbol{y}}$ are the transverse and longitudinal directions, respectively, and the lattice vectors are given by

$$\begin{aligned} \boldsymbol{a}_1 &= L\hat{\boldsymbol{x}}, \\ \boldsymbol{a}_2 &= \frac{1}{2}L\hat{\boldsymbol{x}} + \frac{\sqrt{3}}{2}L\hat{\boldsymbol{y}}. \end{aligned} \tag{61}$$

This journal is © the Owner Societies 2020

Published on 15 September 2020. Downloaded by Universidade Federal do Rio Grande do Sul on 2/10/2021 7:31:45 PM.

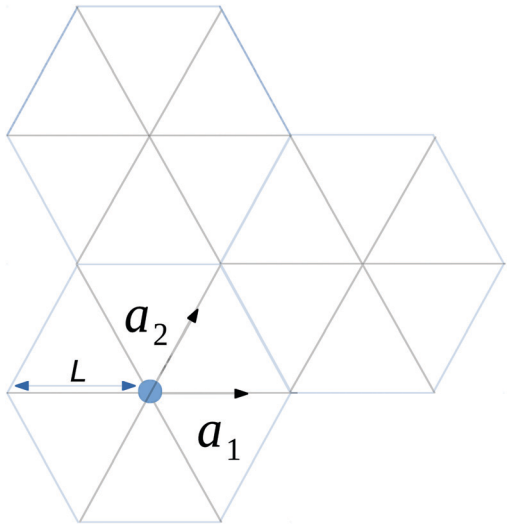

Fig. 11 The triangular lattice used to evaluate μ_c^{qq} and μ_n^{qq}.

The area of the unit cell of triangular lattice is

$$|\gamma| = |\boldsymbol{a}_1 \times \boldsymbol{a}_2| = \frac{\sqrt{3}}{2}L^2 \tag{62}$$

The reciprocal lattice vectors $\boldsymbol{b}_i$ are defined as $\boldsymbol{a}_j \cdot \boldsymbol{b}_j = 2\pi\delta_{ij}$, and are given by

$$\begin{aligned} \boldsymbol{b}_1 &= \frac{2\pi}{L}\left(\hat{\boldsymbol{x}} - \frac{\hat{\boldsymbol{y}}}{\sqrt{3}}\right). \\ \boldsymbol{b}_2 &= \frac{2\pi}{L}\left(\frac{2\hat{\boldsymbol{y}}}{\sqrt{3}}\right). \end{aligned} \tag{63}$$

The periodic delta function can be written as

$$\sum_{n,m}\delta(\boldsymbol{\rho} - n\boldsymbol{a}_1 - m\boldsymbol{a}_2) = \frac{1}{\gamma}\sum_{n,m} e^{i\boldsymbol{b}_1\cdot\boldsymbol{\rho}n + i\boldsymbol{b}_2\cdot\boldsymbol{\rho}m} \tag{64}$$

and the Green function as[100]

$$G(\boldsymbol{r}) = \frac{1}{\gamma}\sum_{n,m} g_{n,m}(z) e^{i\boldsymbol{b}_1\cdot\boldsymbol{\rho}n + i\boldsymbol{b}_2\cdot\boldsymbol{\rho}m}, \tag{65}$$

where $g_{n,m}(z)$ is a function of z coordinate only. Substituting eqn (65) into eqn (60), we obtain

$$\begin{aligned} \frac{\partial^2 g_{n,m}(z)}{\partial z^2} - k^2 g_{n,m}(z) &= -\frac{4\pi q}{\varepsilon_w}\delta(z), \\ k &= \sqrt{\frac{4\pi^2}{L^2}\left(n^2 + \left(\frac{2m}{\sqrt{3}} - \frac{n}{\sqrt{3}}\right)^2\right)}, \end{aligned} \tag{66}$$

which has a solution of the form

$$g_{n,m}(z) = \begin{cases} Ae^{-kz}, & z > 0, \\ Ae^{kz}, & z < 0, \end{cases} \tag{67}$$

Integrating eqn (66) once, we see that the derivative of $g(z)$ is discontinuous at $z = 0$ with

$$g'_{n,m}(0^+) - g'_{n,m}(0^-) = -\frac{4\pi q}{\varepsilon_w}, \tag{68}$$

from which we determine $A = 2\pi q/\varepsilon_w k$,. The Green function can then be written as

$$G(\boldsymbol{r}) = \frac{2\pi q}{\gamma\varepsilon_w}\sum_{n=-\infty}^{n=\infty}\sum_{m=-\infty}^{m=\infty}\frac{e^{-k|z|}}{k}\cos\frac{2\pi}{L}\left(nx + \frac{1}{\sqrt{3}}(2ym - yn)\right). \tag{69}$$

The $(n = 0, m = 0)$ term of $G(\boldsymbol{r})$ diverges. Indeed, if we take the limit $k \to 0$ of the summand in eqn (69), we will obtain an infinite constant and a finite term which grows as $|z|$. This is nothing more than the potential of a uniformly charged plane. Therefore, if we introduce a neutralizing background, we will cancel precisely this term, eliminating the divergence. The electrostatic potential produced by a triangular array of charges on a neutralizing background is then

$$\bar{G}(\boldsymbol{r}) = \frac{2\pi q}{\gamma\varepsilon_w}\sum_{n=-\infty}^{n=\infty'}\sum_{m=-\infty}^{m=\infty'}\frac{e^{-k|z|}}{k}\cos\frac{2\pi}{L}\left(nx + \frac{1}{\sqrt{3}}(2ym - yn)\right), \tag{70}$$

where the prime on the sums indicates that we have removed the terms ($n = 0$ and $m = 0$). Bringing an ion of opposite charge into contact with one of the adsorption sites then yields

$$\mu_c^{qq} = -\frac{2\pi q^2}{\gamma\varepsilon_w}\sum_{n=-\infty}^{n=\infty'}\sum_{m=-\infty}^{m=\infty'}\frac{e^{-2kr_{ion}}}{k}. \tag{71}$$

Even if sites are not perfectly ordered on the colloidal surface, we still expect that μ_c^{qq} derived in eqn (71) will provide a reasonably accurate account of the discreteness effects assuming that the average separation between Z acid sites is such that the area per site is $\gamma = 4\pi(a + r_{ion})^2/Z$, where γ is given by eqn (62). The average separation between acid groups is then $L = (a + r_{ion})\sqrt{8\pi/\sqrt{3}Z}$.

We first consider colloidal particles with 600 acid surface groups with l_g = 109.97 Å, in a solution of pH = 2. The ionic density profiles are presented in Fig. 12. We see that the theory is in excellent agreement with simulations, while the NP

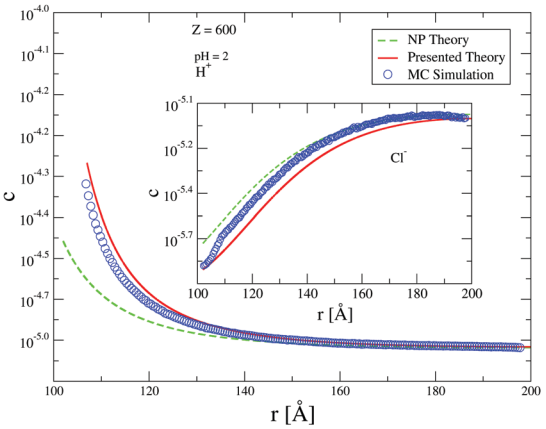

Fig. 12 Comparison between the present theory (solid lines), NP theory (dashed lines) and simulations (symbols), for colloidal particles with Z = 600 and l_g = 109.97 Å functional groups. The densities are in units of particles per Å^3.

Published on 15 September 2020. Downloaded by Universidade Federal do Rio Grande do Sul on 2/10/2021 7:31:45 PM.

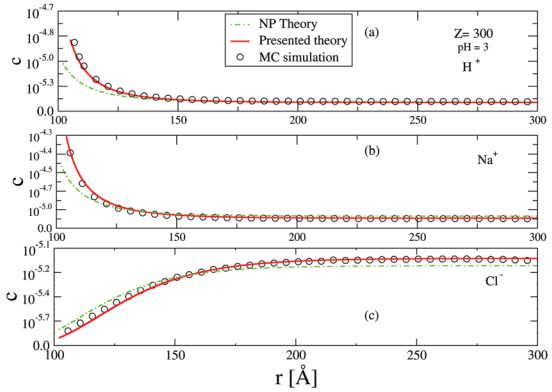

Fig. 13 Comparison between the present theory (solid lines), NP theory (dashed lines) and simulations (symbols), for colloidal particles with Z = 300 charged functional groups with l_g = 109.97 Å. Solution is at pH = 3 and has a 10 mM bulk 1 : 1 salt concentration. The densities are in units of particles per Å^3.

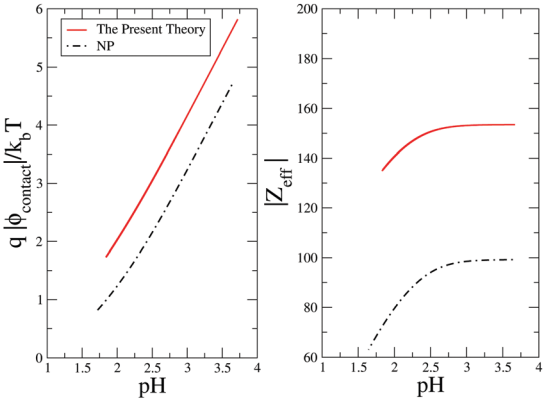

Fig. 15 The modulus of the effective charge in units of q and the contact potential of a nanoparticle as a function of pH in the acid reservoir, predicted by the NP and the present theories. The colloidal particle has 300 charged functional groups on its surface. The parameters are a = 100 Å, R = 200 Å, and l_g = 109.97 Å. The system is salt-free.

approach shows significant deviation. Next we consider particles with 300 charged sites inside an acid solution containing 1 : 1 salt. Once again there is good agreement between theory and simulations, see Fig. 13.

In Fig. 14 we show the behavior of the effective charge and contact potential of colloidal particles as a function of 1 : 1 salt concentration for different pH values.

The figure shows that the increase of salt concentration leads to the increase of the modulus of the effective charge. This, again, is a consequence of electrostatic screening produced by salt on the Coulomb interaction between hydronium ions and the negatively charged adsorption sites – making the association of a hydronium with an active site less energetically favorable. In Fig. 15 we compare the effective charge and contact potential calculated using the present theory and the values predicted by the NP theory, for nanoparticles with 300 charged groups. As can be seen, the neglect of discrete charge effects in the NP theory leads to smaller modulus of the contact potential and of the effective charge. We also note that at large pH the effective charge saturates at a value smaller than the bare charge. This is a consequence of the overall charge neutrality of the colloidal suspension. Even if the reservoir has a very small concentration of acid, large pH, in the absence of other cations inside the suspension, there must be enough hydronium ions to compensate for all the colloidal charge. Some of these hydronium ions will then associate with the surface groups, leading to the saturation of the effective colloidal charge.

We now perform the same calculation, but in the presence of a reservoir with 10 mM monovalent salt. As can be seen in Fig. 16, in the presence of salt, for high pH, both NP and our theory predict that the effective charge approaches the bare charge. This is in contrast with the no-salt system. When the system is connected to both the salt and acid reservoirs, at large pH, the hydronium ions inside the system are replaced by the salt cations, which then control the overall charge neutrality of

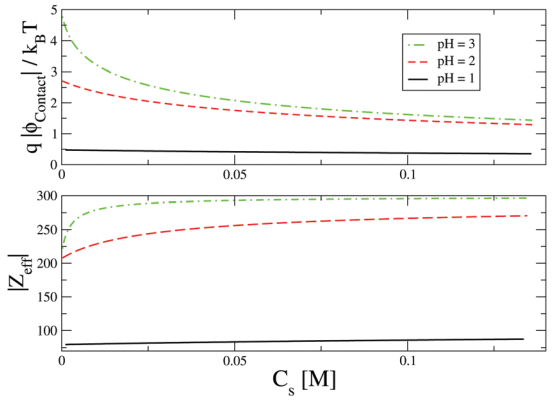

Fig. 14 Modulus of the effective charge in units of q and contact potential of colloidal particles as a function of 1 : 1 salt concentration C_s for different values of pH. The colloidal particle has 300 charged functional groups on its surface. The parameters are a = 100 Å, R = 200 Å, and l_g = 109.97 Å. The densities are in units of particles per Å^3.

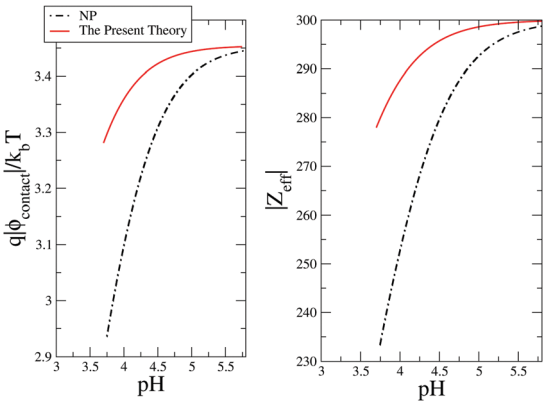

Fig. 16 The modulus of the effective charge in units of q and the contact potential of a nanoparticle as a function of pH in the acid reservoir, predicted by the NP and the present theories. The colloidal particle has 300 charged functional groups on its surface. The suspension is in contact with a monovalent salt reservoir at concentration of 10 mM. The parameters are a = 100 Å, R = 200 Å, and l_g = 109.97 Å.

This journal is © the Owner Societies 2020

Published on 15 September 2020. Downloaded by Universidade Federal do Rio Grande do Sul on 2/10/2021 7:31:45 PM.

the colloidal suspension. Since in our model salt cations do not react with the surface groups, for reservoir at large pH, very few hydronium ions will be present inside the suspension. Therefore, all the surface groups will become ionized, and the effective colloidal charge will approach the value of the bare charge.

VIII. Mixture of functional groups

As a final example, we consider a colloidal particle with a mixture of acidic and basic surface groups. Following the same approach introduced in the previous sections we find that the effective surface charge is

$$\begin{aligned}\sigma_{\text{eff}} &= -\frac{N_{\text{acid}}q}{4\pi(a+r_{\text{ion}})^2}+q\left(l_{\text{gc}}^{\text{eff}}c_{\text{a}}\text{e}^{-\beta\varphi_0^{\text{c}}}+l_{\text{gn}}^{\text{eff}}c_{\text{a}}\text{e}^{-\beta\varphi_0^{\text{n}}}\right),\\ l_{\text{gc}}^{\text{eff}} &= \frac{l_{\text{gc}}N_{\text{acid}}{r_{\text{patch}}}^2}{4(a+r_{\text{ion}})^2\left(1+l_{\text{gc}}c_{\text{a}}\text{e}^{-\beta\varphi_0^{\text{c}}}\pi{r_{\text{patch}}}^2\right)},\\ l_{\text{gn}}^{\text{eff}} &= \frac{l_{\text{gn}}N_{\text{base}}{r_{\text{patch}}}^2}{4(a+r_{\text{ion}})^2\left(1+l_{\text{gn}}c_{\text{a}}\text{e}^{-\beta\varphi_0^{\text{n}}}\pi{r_{\text{patch}}}^2\right)},\end{aligned}\tag{72}$$

where N_{acid} is the number of acidic groups and $N_{\text{base}} = N_{\text{site}} - N_{\text{acid}}$ is the number of basic groups. The effective sticky length for acidic (charged) and basic (neutral) groups are: $l_{\text{gc}}^{\text{eff}}$ and $l_{\text{gn}}^{\text{eff}}$, respectively. The discreteness effects will manifest themselves in different ways for hydronium ions condensing on acidic and basic groups,

$$\begin{aligned}\beta\varphi_0^{\text{c}} &= \beta\phi_0^{\text{c}}+\mu_{\text{c}}^{\text{qq}},\\ \beta\varphi_0^{\text{n}} &= \beta\phi_0^{\text{n}}+\mu_{\text{n}}^{\text{qq}},\end{aligned}\tag{73}$$

Since the values $\mu_{\text{c,n}}^{\text{qq}}$ depend only on the electrostatic interaction between the hydronium ions and the charged (acid) sites, the value of $\mu_{\text{c}}^{\text{qq}}$ will be the same as in eqn (71), depending only on the average separation between the acidic groups. We will suppose that the basic groups are also uniformly distributed on the colloidal surface on a dual hexagonal lattice with vertexes at the center of each triangle composed of acidic sites. In this case the position of one of the basic groups will be at $x_0 = d/2$, $y_0 = \sqrt{3d}/4$. Using eqn (70) we obtain $\mu_{\text{n}}^{\text{qq}}$

$$\mu_{\text{n}}^{\text{qq}} = -\frac{2\pi q^2}{\gamma\varepsilon_{\text{w}}}\sum_{n=-\infty}^{n=\infty'}\sum_{m=-\infty}^{m=\infty'}\frac{\text{e}^{-2kr_{\text{ion}}}}{k}\cos\pi\left(m+\frac{n}{2}\right)\tag{74}$$

The effective surface charge density can now be written as

$$\begin{aligned}\sigma_{\text{eff}} &= -\frac{N_{\text{acid}}q}{4\pi(a+r_{\text{ion}})^2}+\frac{qK_{\text{Surf}}^{\text{a}}N_{\text{acid}}c_{\text{a}}\text{e}^{-\beta\phi_0}}{4\pi(a+r_{\text{ion}})^2\left(1+K_{\text{Surf}}^{\text{a}}c_{\text{a}}\text{e}^{-\beta\phi_0}\right)}\\ &\quad+\frac{qK_{\text{Surf}}^{\text{b}}N_{\text{base}}c_{\text{a}}\text{e}^{-\beta\phi_0}}{4\pi(a+r_{\text{ion}})^2\left(1+K_{\text{Surf}}^{\text{b}}c_{\text{a}}\text{e}^{-\beta\phi_0}\right)}\end{aligned}\tag{75}$$

where

$$K_{\text{Surf}}^{\text{a}} = \frac{K_{\text{Bulk}}^{\text{a}}}{2}\text{e}^{-b-\beta\mu_{\text{c}}^{\text{qq}}},\tag{76}$$

and

$$K_{\text{Surf}}^{\text{b}} = \frac{K_{\text{Bulk}}^{\text{b}}}{2}\text{e}^{-\beta\mu_{\text{n}}^{\text{qq}}}.\tag{77}$$

The bulk equilibrium constants for acid and base, $K_{\text{Bulk}}^{\text{a}}$ and $K_{\text{Bulk}}^{\text{b}}$, are given by eqn (43) and (35), respectively. To test our theory for mixture of basic and acidic surface groups we, once again, compare it with MC simulations. We consider a colloidal particle with 500 adsorption sites with different numbers of acidic groups N_{acid}. The sticky lengths – l_{gc} and l_{gn} – are 109.97 and 1099.7, respectively. These values correspond to the equilibrium constants K_{a} = 0.012 and 0.00125 M, respectively. The concentration of strong acid, HCl, in the reservoir is fixed at 10 mM. We note that as the value of the sticky length l_{g} increases, it becomes progressively more difficult to equilibrate the simulations. For this reason we have chosen values of l_{g} that are not too large. This, however, has no implication for the theory, which remains valid for arbitrary values of l_{g} and K_{a}.

Since the theory is completely general, the values of l_{g} are arbitrarily and one can, in practice, choose the depth and the width of the sticky potential and calculate the sticky length. There is, however, an additional constraint. The equilibration of the simulations becomes progressively more difficult with the increase of the sticky length. To have a good test of the theory we, therefore, need to choose a sufficiently large sticky length to have a significant association of hydronium ions with the adsorption sites, while keeping a reasonable equilibration CPU time. Furthermore, to better test the validity of the theory, we should choose very different sticky lengths for acid and base sites. This is the reason for a factor of 10 difference between the values of l_{g} of acidic and basic groups. In Table 1 we show the values of $\mu_{\text{c}}^{\text{qq}}$ and $\mu_{\text{n}}^{\text{qq}}$, calculated using eqn (71) and (74), respectively – for a colloidal particle with the total of N_{site} = 500 adsorption sites, N_{acid} of which are acidic (charged) and the rest are basic.

Fig. 17 shows that for a small number of basic sites, the theory remains very accurate. This is also the case if the number of basic sites is significantly larger than the number of acidic sites. The worst agreement is found when $N_{\text{acid}} \approx N_{\text{base}}$ in which case the surface of the colloid becomes strongly heterogeneous, with positive, negative, and neutral domains present, leading to the breakdown of assumptions used to calculate $\mu_{\text{c,n}}^{\text{qq}}$.

From the obtained results, we conclude that the theory works very well if the colloidal particle has either basic or acidic adsorption sites. The discrete charge effects are embedded in the $\mu_{\text{c}}^{\text{qq}}$ and $\mu_{\text{n}}^{\text{qq}}$, which are calculated using a regular arrangement of adsorption sites, even though in the simulations the sites are randomly distributed. If the number of acid and base sites is approximately equal, then after the adsorption, we will end up

Table 1 Different values of $\mu_{\text{c}}^{\text{qq}}$ and $\mu_{\text{n}}^{\text{qq}}$ for a mixture of charged sites. The total number of adsorption sites is 500

N_{acid}	500	450	300	200	50
$\mu_{\text{c}}^{\text{qq}}$	−0.6278	−0.6653	−0.8073	−0.94227	−1.31329
$\mu_{\text{n}}^{\text{qq}}$	—	0.14311	0.1519	0.1529	0.119273

Published on 15 September 2020. Downloaded by Universidade Federal do Rio Grande do Sul on 2/10/2021 7:31:45 PM.

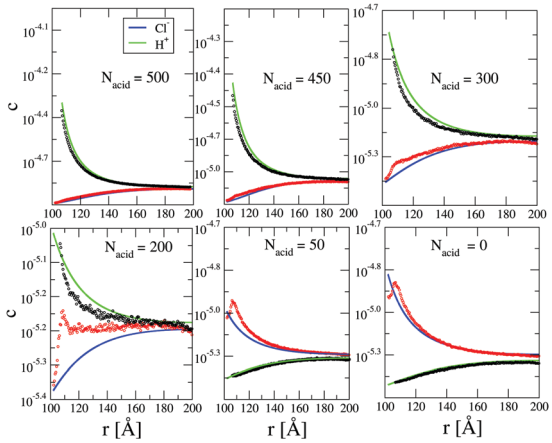

Fig. 17 Density profiles of ions around colloidal particles with different numbers of charged and neutral functional groups. The total number of sites is N_{site} = 500, the pH of the reservoir is 2 and there is no additional salt. Symbols denote the results of MC simulations and the lines are predictions of the theory. The densities are in units of particles per Å^3.

with large domains composed of −1, 0, +1 charges, and our assumptions for calculating μ_c^{qq} and μ_n^{qq} will break down. Nevertheless the theory is found to work quite well, as long as the number of acidic and basic sites is not the same. The addition of salt to the system results in even better agreement between theory and simulations. Therefore, the salt free case provides the most stringent test of the theoretical approach.

IX. Conclusion

In this work, we used a sticky sphere model to mimic chemical reactions on a colloidal surface. Within our theory, the discrete charge effects come only from acid surface sites, since ions are treated at the mean field Poisson–Boltzmann level. This is the reason why the surface equilibrium constant is dependent only on the value of μ^{qq}. In the previous work we studied colloidal particles with only acidic surface groups.[16] In that approach we used one component plasma model (OCP), to account for the electrostatic corrections due to discrete surface groups. While the approach in ref. 16 was sufficiently accurate for colloidal particles with only acidic groups, the OCP does not take into account the ionic radius, which prevented us from extending this approach to colloidal particles with a mixture of acidic and basic surface groups. In the present study, we have developed a completely different method to account for discrete surface effects using periodic Green functions. The fact that this theory works well even for very small nanoparticles of 10 nm radius shows the robustness of our approach.

The microscopic model presented in the paper permits us to study the same chemical reaction taking place in bulk and at the interface. In the case of neutral basic surface groups our theory reduces to the NP approach with the bulk equilibrium constant replaced by the surface equilibrium constant,

$$K_{Surf}^{b} \to \frac{1}{2} K_{Bulk}^{b}. \tag{78}$$

The difference between surface and bulk equilibrium constants is a consequence of steric repulsion, which restricts the overall surface area of the adsorption sites available for interaction with hydronium ions.

For colloidal particles with acidic surface groups the situation is significantly more complex. In this case our theory reduces to the NP approach with an effective surface equilibrium constant only for weak acidic groups. For such systems we find the surface equilibrium constant to be

$$K_{Surf}^{a} = \frac{K_{Bulk}^{a}}{2} e^{-b-\beta\mu_c^{qq}}, \tag{79}$$

where μ_c^{qq} accounts for the discreteness of the surface charge. For colloidal particles with a mixture of acidic and basic surface groups, the respective surface equilibrium constants are given by eqn (76) and (77).

It is important to stress that eqn (78) and (79) are not universal, and in general, will depend on the details of the system. These details may include molecular geometry, modified electronic structure of surface functional groups, water structure, *etc.* Nevertheless the model of sticky adsorption sites demonstrates that there is a mapping between the bulk and the surface equilibrium constants which allows one to use the Poisson–Boltzmann framework to accurately account for the charge regulation in colloidal systems. Any deviations from the experiment can therefore be attributed to the shortfall of the model and not to the theoretical method used to solve it.

In this work, our primary goal was to explore the extent of validity of the mean-field NP approach by applying it to an exactly solvable model. Clearly the microscopic model that we used for spherically symmetric hydronium, uniform dielectric water, sticky interactions for covalent binding, *etc.*, is a very rough approximation to the physical reality. The advantage is that we can solve this model exactly using computer simulations. By applying the NP approach to the same model we can then test the extent of validity of the mean-field approximations. We should stress that the NP theory does not give us any information whatsoever about the surface equilibrium constant and assumes it to be the same as the bulk association constant. We find, on the other hand, that sticky interactions result in a breakdown of the mean-field approximations. Surprisingly, however, we observe that all the discreteness effects can be included in a renormalized surface association constant, which our theory predicts explicitly. For our microscopic model the correlations and steric effects lead to lower surface association constant K_{Surf}, compared to the bulk association constant for the same acid or base, K_{Bulk}. This means that fewer hydronium ions will bind to surface groups, implying that surface pK_a will be smaller than bulk pK_a. Within the present model, there are two contributions which account for the decrease of the association constant at the surface. The first is the steric repulsion from the colloidal surface, which diminishes the access of hydronium to acid and base groups. Within our model the accessible area for the charge transfer reaction is lowered by a factor of two, which accounts for a factor of 1/2 in the surface binding constant. The second contribution comes from the

 This journal is © the Owner Societies 2020

Published on 15 September 2020. Downloaded by Universidade Federal do Rio Grande do Sul on 2/10/2021 7:31:45 PM.

discrete nature of surface charged groups, which we also find to lower the effective binding constant. On the other hand, the experiments indicate that the surface binding constant, K_{Surf}, that one needs to use in the NP theory is actually larger than K_{Bulk}. This means that the surface pK_a is larger than the pK_a of the bulk acid.[101] Since our model already takes into account all the steric and electrostatic effects at the dielectric continuum level, we must conclude that in order to account for the experimental results we must include additional effects into the model, such as dielectric discontinuity across the colloidal structure, water ordering, quantum nature of proton transfer, *etc.* The approach that we have developed should allow us to explore these additional effects in order to understand the mechanisms that lead to the increase of pK_a at the colloidal surface. This will be the subject of the future work.

Conflicts of interest

There are no conflicts to declare.

Acknowledgements

This work was partially supported by the CNPq.

References

1 C. Rønne, L. Thrane, P.-O. Åstrand, A. Wallqvist, K. V. Mikkelsen and S. R. Keiding, Investigation of the temperature dependence of dielectric relaxation in liquid water by thz reflection spectroscopy and molecular dynamics simulation, *J. Chem. Phys.*, 1997, **107**(14), 5319–5331.
2 D. Andelman, Chapter 12 - electrostatic properties of membranes: the Poisson-Boltzmann theory, in *Structure and Dynamics of Membranes. vol. 1 of Handbook of Biological Physics*, ed. R. Lipowsky and E. Sackmann, North-Holland, 1995, pp. 603–642.
3 R. Messina, Electrostatics in soft matter, *J. Phys.: Condens. Matter*, 2009, **21**, 113102.
4 A. Abrashkin, D. Andelman and H. Orland, Dipolar Poisson-Boltzmann equation: Ions and dipoles close to charge interfaces, *Phys. Rev. Lett.*, 2007, **99**, 077801.
5 Y. Levin, Electrostatic correlations: from plasma to biology, *Rep. Prog. Phys.*, 2002, **65**(11), 1577.
6 K. Shen and Z.-G. Wang, Electrostatic correlations and the polyelectrolyte self energy, *J. Chem. Phys.*, 2017, **146**(8), 084901.
7 A. M. Smith, A. A. Lee and S. Perkin, The electrostatic screening length in concentrated electrolytes increases with concentration, *J. Phys. Chem. Lett.*, 2016, **7**(12), 2157–2163.
8 R. M. Adar, T. Markovich, A. Levy, H. Orland and D. Andelman, Dielectric constant of ionic solutions: Combined effects of correlations and excluded volume, *J. Chem. Phys.*, 2018, **149**(5), 054504.
9 M. I. Bespalova, S. Mahanta and M. Krishnan, Single-molecule trapping and measurement in solution, *Curr. Opin. Chem. Biol.*, 2019, **51**, 113–121. Chemical Genetics and Epigenetics Molecular Imaging.
10 D. Frydel, S. Dietrich and M. Oettel, Charge renormalization for effective interactions of colloids at water interfaces, *Phys. Rev. Lett.*, 2007, **99**, 118302.
11 D. A. Walker, B. Kowalczyk, M. O. de La Cruz and B. A. Grzybowski, Electrostatics at the nanoscale, *Nanoscale*, 2011, **3**(4), 1316–1344.
12 S. Alexander, P. Chaikin, P. Grant, G. Morales, P. Pincus and D. Hone, Charge renormalization, osmotic pressure, and bulk modulus of colloidal crystals: Theory, *J. Chem. Phys.*, 1984, **80**(11), 5776–5781.
13 E. Trizac, L. Bocquet and M. Aubouy, Simple approach for charge renormalization in highly charged macroions, *Phys. Rev. Lett.*, 2002, **89**(24), 248301.
14 A. Adamson and A. Gast, *Chemistry of Surfaces*. John Wiley & Sons, New York, NY, USA, 1997.
15 D. Wang, R. J. Nap, I. Lagzi, B. Kowalczyk, S. Han, B. A. Grzybowski and I. Szleifer, How and why nanoparticle's curvature regulates the apparent pka of the coating ligands, *J. Am. Chem. Soc.*, 2011, **133**(7), 2192–2197.
16 A. Bakhshandeh, D. Frydel, A. Diehl and Y. Levin, Charge regulation of colloidal particles: Theory and simulations, *Phys. Rev. Lett.*, 2019, **123**(20), 208004.
17 R. Podgornik, General theory of charge regulation and surface differential capacitance, *J. Chem. Phys.*, 2018, **149**(10), 104701.
18 D. Frydel, General theory of charge regulation within the Poisson-Boltzmann framework: Study of a sticky-charged wall model, *J. Chem. Phys.*, 2019, **150**(19), 194901.
19 Y. Avni, D. Andelman and R. Podgornik, Charge regulation with fixed and mobile charged macromolecules, *Curr. Opin. Electrochem.*, 2019, **13**, 70–77.
20 K. Linderstrøm-Lang, On the ionization of proteins, *CR Trav. Lab. Carlsberg*, 1924, **15**(7), 1–29.
21 A. Majee, M. Bier, R. Blossey and R. Podgornik, Charge regulation radically modifies electrostatics in membrane stacks, *Phys. Rev. E: Stat., Nonlinear, Soft Matter Phys.*, 2019, **100**(5), 050601.
22 Y. Avni, T. Markovich, R. Podgornik and D. Andelman, Charge regulating macro-ions in salt solutions: screening properties and electrostatic interactions, *Soft Matter*, 2018, **14**, 6058–6069.
23 D. Chan, J. PerTam, L. White and T. Healy, Regulation of surface potential at amphoteric surfaces during partiele-particle interaction, *J. Chem. Soc., Faraday Trans.*, 1975, **71**, 1046–1057.
24 R. Pericet-Camara, G. Papastavrou, S. H. Behrens and M. Borkovec, Interaction between charged surfaces on the Poisson-Boltzmann level: The constant regulation approximation, *J. Phys. Chem. B*, 2004, **108**(50), 19467–19475.
25 H. von Grünberg, Chemical charge regulation and charge renormalization in concentrated colloidal suspensions, *J. Colloid Interface Sci.*, 1999, **219**(2), 339–344.
26 H. G. Ozcelik and M. Barisik, Electric charge of nanopatterned silica surfaces, *Phys. Chem. Chem. Phys.*, 2019, **21**(14), 7576–7587.

Published on 15 September 2020. Downloaded by Universidade Federal do Rio Grande do Sul on 2/10/2021 7:31:45 PM.

27 A. Lošdorfer Božič and R. Podgornik, Anomalous multipole expansion: Charge regulation of patchy inhomogeneously charged spherical particles, *J. Chem. Phys.*, 2018, **149**(16), 163307.
28 F. B. van Swol and D. N. Petsev, Solution structure effects on the properties of electric double layers with surface charge regulation assessed by density functional theory, *Langmuir*, 2018, **34**(46), 13808–13820.
29 T. Markovich, D. Andelman and R. Podgornik, Charge regulation: A generalized boundary condition?, *EPL*, 2016, **113**, 26004.
30 M. Krishnan, A simple model for electrical charge in globular macromolecules and linear polyelectrolytes in solution, *J. Chem. Phys.*, 2017, **146**(20), 205101.
31 M. Krishnan, Electrostatic free energy for a confined nanoscale object in a fluid, *J. Chem. Phys.*, 2013, **138**(11), 114906.
32 R. A. Hartvig, M. van de Weert, J. Østergaard, L. Jorgensen and H. Jensen, Protein adsorption at charged surfaces: The role of electrostatic interactions and interfacial charge regulation, *Langmuir*, 2011, **27**(6), 2634–2643.
33 D. C. Prieve and E. Ruckenstein, The surface potential of and double-layer interaction force between surfaces characterized by multiple ionizable groups, *J. Theor. Biol.*, 1976, **56**(1), 205–228.
34 S. L. Carnie and D. Y. Chan, Interaction free energy between plates with charge regulation: a linearized model, *J. Colloid Interface Sci.*, 1993, **161**(1), 260–264.
35 R. Netz, Charge regulation of weak polyelectrolytes at low- and high-dielectric-constant substrates, *J. Phys.: Condens. Matter*, 2002, **15**(1), S239.
36 A. Majee, M. Bier and R. Podgornik, Spontaneous symmetry breaking of charge-regulated surfaces, *Soft Matter*, 2018, **14**, 985–991.
37 J. E. Hallett, D. A. Gillespie, R. M. Richardson and P. Bartlett, Charge regulation of nonpolar colloids, *Soft Matter*, 2018, **14**(3), 331–343.
38 M. Heinen, T. Palberg and H. Löwen, Coupling between bulk- and surface chemistry in suspensions of charged colloids, *J. Chem. Phys.*, 2014, **140**(12), 124904.
39 C.-Y. Leung, L. C. Palmer, S. Kewalramani, B. Qiao, S. I. Stupp, M. Olvera de la Cruz and M. J. Bedzyk, Crystalline polymorphism induced by charge regulation in ionic membranes, *Proc. Natl. Acad. Sci. U. S. A.*, 2013, **110**(41), 16309–16314.
40 G. S. Longo, M. Olvera de la Cruz and I. Szleifer, Molecular theory of weak polyelectrolyte gels: The role of ph and salt concentration, *Macromolecules*, 2011, **44**(1), 147–158.
41 R. Zandi, B. Dragnea, A. Travesset and R. Podgornik, On virus growth and form, *Phys. Rep.*, 2020, **847**, 1–102.
42 D. Roshal, O. Konevtsova, A. L. Božič, R. Podgornik and S. Rochal, ph-induced morphological changes of proteinaceous viral shells, *Sci. Rep.*, 2019, **9**(1), 5341.
43 L. Javidpour, A. L. Božič, R. Podgornik and A. Naji, Role of metallic core for the stability of virus-like particles in strongly coupled electrostatics, *Sci. Rep.*, 2019, **9**(1), 3884.
44 C. T. Zahler and B. F. Shaw, What are we missing by not measuring the net charge of proteins?, *Chem. – Eur. J.*, 2019, **25**(32), 7581–7590.
45 A. L. Božič and R. Podgornik, ph dependence of charge multipole moments in proteins, *Biophys. J.*, 2017, **113**(7), 1454–1465.
46 M. Lund, T. Åkesson and B. Jönsson, Enhanced protein adsorption due to charge regulation, *Langmuir*, 2005, **21**(18), 8385–8388.
47 H. Shen and D. D. Frey, Effect of charge regulation on steric mass-action equilibrium for the ion-exchange adsorption of proteins, *J. Chromatogr. A*, 2005, **1079**(1), 92–104.
48 P. M. Biesheuvel and A. Wittemann, A modified box model including charge regulation for protein adsorption in a spherical polyelectrolyte brush, *J. Phys. Chem. B*, 2005, **109**(9), 4209–4214.
49 N. S. Pujar and A. L. Zydney, Charge regulation and electrostatic interactions for a spherical particle in a cylindrical pore, *J. Colloid Interface Sci.*, 1997, **192**(2), 338–349.
50 Y. Burak and R. R. Netz, Charge regulation of interacting weak polyelectrolytes, *J. Phys. Chem. B*, 2004, **108**(15), 4840–4849.
51 R. Kumar, B. G. Sumpter and S. M. Kilbey, Charge regulation and local dielectric function in planar polyelectrolyte brushes, *J. Chem. Phys.*, 2012, **136**(23), 234901.
52 C. Fleck, R. R. Netz and H. H. von Grünberg, Poisson-Boltzmann theory for membranes with mobile charged lipids and the ph-dependent interaction of a dna molecule with a membrane, *Biophys. J.*, 2002, **82**(1), 76–92.
53 M. Lund and B. Jönsson, Charge regulation in biomolecular solution, *Q. Rev. Biophys.*, 2013, **46**, 265–281.
54 M. L. Grant, Nonuniform charge effects in protein-protein interactions, *J. Phys. Chem. B*, 2001, **105**, 2858–2863.
55 A. H. Elcock and J. A. McCammon, Calculation of weak protein-protein interactions: The pH dependence of the second virial coefficient, *Biophys. J.*, 2001, **80**, 613–625.
56 M. Lund and B. Jönsson, On the Charge Regulation of Proteins, *Biochemistry*, 2005, **44**(15), 5722–5727.
57 A. C. Mason and J. H. Jensen, Protein-protein binding is often associated with changes in protonation state, *Proteins: Struct., Funct., Bioinf.*, 2008, **71**, 81–91.
58 B. Aguilar, R. Anandakrishnan, J. Z. Ruscio and A. V. Onufriev, Statistics and physical origins of pK and ionization state changes upon protein-ligand binding, *Biophys. J.*, 2010, **98**, 872–880.
59 J. Ståhlberg and B. Jönsson, Influence off charge regulation in electrostatic interaction chromatography of proteins, *Anal. Chem.*, 1996, **68**(9), 1536–1544.
60 H. K. Tsao, Electrostatic interaction of an assemblage of charges with a charged surface: the charge-regulation effect, *Langmuir*, 2000, **16**, 7200–7209.
61 A. Kubincová, P. H. Hünenberger and M. Krishnan, Interfacial solvation can explain attraction between like-charged

 This journal is © the Owner Societies 2020

Published on 15 September 2020. Downloaded by Universidade Federal do Rio Grande do Sul on 2/10/2021 7:31:45 PM.

objects in aqueous solution, *J. Chem. Phys.*, 2020, **152**(10), 104713.
62 T. Markovich, D. Andelman and R. Podgornik, Complex fluids with mobile charge-regulating macro-ions, *EPL*, 2017, **120**, 26001.
63 R. Podgornik and V. Parsegian, An electrostatic-surface stability interpretation of the hydrophobic force inferred to occur between mica plates in solutions of soluble surfactants, *Chem. Phys.*, 1991, **154**(3), 477–483.
64 D. Leckband and J. Israelachvili, Intermolecular forces in biology, *Q. Rev. Biophys.*, 2001, **34**(2), 105–267.
65 G. Trefalt, S. H. Behrens and M. Borkovec, Charge regulation in the electrical double layer: Ion adsorption and surface interactions, *Langmuir*, 2016, **32**(2), 380–400.
66 P. M. Biesheuvel, M. van der Veen and W. Norde, A modified Poisson-Boltzmann model including charge regulation for the adsorption of ionizable polyelectrolytes to charged interfaces, applied to lysozyme adsorption on silica, *J. Phys. Chem. B*, 2005, **109**(9), 4172–4180.
67 J.-P. Hsu and B.-T. Liu, Stability of colloidal dispersions: Charge regulation/adsorption model, *Langmuir*, 1999, **15**(16), 5219–5226.
68 J. K. Wolterink, L. Koopal, M. C. Stuart and W. V. Riemsdijk, Surface charge regulation upon polyelectrolyte adsorption, hematite, polystyrene sulfonate, surface charge regulation: Theoretical calculations and hematite-poly(styrene sulfonate) system, *Colloids Surf., A*, 2006, **291**(1), 13–23.
69 I. Popa, G. Papastavrou and M. Borkovec, Charge regulation effects on electrostatic patch-charge attraction induced by adsorbed dendrimers, *Phys. Chem. Chem. Phys.*, 2010, **12**, 4863–4871.
70 P. Gong, J. Genzer and I. Szleifer, Phase behavior and charge regulation of weak polyelectrolyte grafted layers, *Phys. Rev. Lett.*, 2007, **98**, 018302.
71 S. H. Behrens and M. Borkovec, Exact Poisson-Boltzmann solution for the interaction of dissimilar charge-regulating surfaces, *Phys. Rev. E: Stat. Phys., Plasmas, Fluids, Relat. Interdiscip. Top.*, 1999, **60**, 7040–7048.
72 J. G. Kirkwood and J. B. Shumaker, The influence of dipole moment fluctuations on the dielectric increment of proteins in solution, *Proc. Natl. Acad. Sci. U. S. A.*, 1952, **38**(10), 855.
73 R. Marcus, Calculation of thermodynamic properties of polyelectrolytes, *J. Chem. Phys.*, 1955, **23**(6), 1057–1068.
74 S. Lifson, Potentiometric titration, association phenomena, and interaction of neighboring groups in polyelectrolytes, *J. Chem. Phys.*, 1957, **26**(4), 727–734.
75 N. Adžić and R. Podgornik, Field-theoretic description of charge regulation interaction, *Eur. Phys. J. E: Soft Matter Biol. Phys.*, 2014, **37**, 49.
76 A. M. Smith, M. Borkovec and G. Trefalt, Forces between solid surfaces in aqueous electrolyte solutions, *Adv. Colloid Interface Sci.*, 2020, **275**, 102078.
77 C. Safinya and J. Radler, *Handbook of Lipid Membranes: Molecular, Functional, and Materials Aspects*, Taylor & Francis, 2014.
78 B. W. Ninham and V. A. Parsegian, Electrostatic potential between surfaces bearing ionizable groups in ionic equilibrium with physiologic saline solution, *J. Theor. Biol.*, 1971, **31**(3), 405–428.
79 D. L. Chapman, Li. a contribution to the theory of electrocapillarity, *London Edinburgh Philos. Mag. J. Sci.*, 1913, **25**(148), 475–481.
80 M. Gouy, Sur la constitution de la charge électrique à la surface d'un électrolyte, *Ann. Phys.*, 1910, **9**, 457–468.
81 R. Baxter, Percus-Yevick equation for hard spheres with surface adhesion, *J. Chem. Phys.*, 1968, **49**(6), 2770–2774.
82 D. Frydel, One-dimensional coulomb system in a sticky wall confinement: Exact results, *Phys. Rev. E: Stat., Nonlinear, Soft Matter Phys.*, 2019, **100**, 042113.
83 M. A. Miller and D. Frenkel, Competition of percolation and phase separation in a fluid of adhesive hard spheres, *Phys. Rev. Lett.*, 2003, **90**, 135702.
84 G. Foffi, C. D. Michele, F. Sciortino and P. Tartaglia, Scaling of dynamics with the range of interaction in short-range attractive colloids, *Phys. Rev. Lett.*, 2005, **94**, 078301.
85 J. N. Herrera and L. Blum, Sticky electrolyte mixtures in the Percus-Yevick/mean spherical approximation, *J. Chem. Phys.*, 1991, **94**(7), 5077–5082.
86 L. Blum, M. L. Rosinberg and J. P. Badiali, Contact theorems for models of the sticky electrode, *J. Chem. Phys.*, 1989, **90**(2), 1285–1286.
87 D. A. Huckaby and L. Blum, Exact results for the adsorption of a dense fluid onto a triangular lattice of sticky sites, *J. Chem. Phys.*, 1990, **92**(4), 2646–2649.
88 J. A. Greathouse and D. A. McQuarrie, Conventional hypernetted chain force calculations for charged plates with adsorbing counterions, *J. Colloid Interface Sci.*, 1996, **181**(1), 319–325.
89 J. A. Greathouse and D. A. McQuarrie, *J. Phys. Chem.*, 1996, **100**(5), 1847–1851.
90 M. S. Wertheim, Fluids with highly directional attractive forces. IV. Equilibrium polymerization, *J. Stat. Phys.*, 1986, **42**, 477–492.
91 Y. Wang, Y. Wang, D. R. Breed, V. N. Manoharan, L. Feng, A. D. Hollingsworth, M. Weck and D. J. Pine, Colloids with valence and specific directional bonding, *Nature*, 2012, **491**, 51–55.
92 M. N. Tamashiro, Y. Levin and M. C. Barbosa, Donnan equilibrium and the osmotic pressure of charged colloidal lattices, *Eur. Phys. J. B*, 1998, **1**(3), 337–343.
93 N. Metropolis, A. W. Rosenbluth, M. N. Rosenbluth, A. H. Teller and E. Teller, Equation of state calculations by fast computing machines, *J. Chem. Phys.*, 1953, **21**(6), 1087–1092.
94 D. Frenkel and B. Smith, *Understanding Molecular Simulation*, Academic Press, New York, 1996.
95 T. Hill, *Statistical Mechanics: Principles and Selected Applications*, Dover Publications Inc., New York, 1987.
96 D. A. McQuarrie, *Statistical Mechanics*, Harper's Chemistry Series, HarperCollins Publishing, Inc., New York, 1976.

Published on 15 September 2020. Downloaded by Universidade Federal do Rio Grande do Sul on 2/10/2021 7:31:45 PM.

97 W. Ebeling, Zur theorie der bjerrumschen ionenassoziation in elektrolyten, *Z. Phys. Chem.*, 1968, **238**(1), 400–402.
98 H. Falkenhagen and W. Ebeling, *Equilibrium Properties of Ionized Dilute Electrolytes*, Academic Press, New York, 1971.
99 Y. S. Jho, S. A. Safran, M. In and P. A. Pincus, Effect of charge inhomogeneity and mobility on colloid aggregation, *Langmuir*, 2012, **28**(22), 8329–8336.
100 A. P. dos Santos, M. Girotto and Y. Levin, Simulations of coulomb systems confined by polarizable surfaces using periodic green functions, *J. Chem. Phys.*, 2017, **147**(18), 184105.
101 S. H. Behrens, D. I. Christl, R. Emmerzael, P. Schurtenberger and M. Borkovec, Charging and aggregation properties of carboxyl latex particles:experiments *versus* dlvo theory, *Langmuir*, 2000, **16**(6), 2566–2575.

 This journal is © the Owner Societies 2020